

Real-time study of the adiabatic energy loss in an atomic collision with a metal cluster

Roi Baer and Nidal Siam

*Department of Physical Chemistry, The Hebrew University of Jerusalem, Jerusalem 91904, Israel
and the Lise Meitner Minerva-Center for Quantum Chemistry, The Hebrew University of Jerusalem,
Jerusalem 91904, Israel*

(Received 7 May 2004; accepted 12 July 2004)

Gas-phase hydrogen atoms are accelerated towards metallic surfaces in their vicinity. As it approaches the surface, the velocity of an atom increases and this motion excites the metallic electrons, causing energy loss to the atom. This dissipative dynamics is frequently described as atomic motion under friction, where the friction coefficient is obtained from *ab initio* calculations assuming a weak interaction and slow atom. This paper tests the aforementioned approach by comparing to a real-time Ehrenfest molecular dynamics simulation of such a process. The electrons are treated realistically using standard approximations to time-dependent density functional theory. We find indeed that the electronic excitations produce a frictionlike force on the atom. However, the friction coefficient strongly depends on the *direction* of the motion of the atom: it is large when the atom is moving towards the cluster and much smaller when the atom is moving away. It is concluded that a revision of the model for energy dissipation at metallic surfaces, at least for clusters, may be necessary. © 2004 American Institute of Physics. [DOI: 10.1063/1.1788658]

I. INTRODUCTION

Gas-surface interactions form one of the most active fields of molecular physics and chemistry, with key applications in catalysis, microelectronics, and environmental chemistry. In recent years a lot of interest has arisen in the role of small metal cluster surfaces, as these have unique chemical properties, absent or different from those of the surface of a bulk. Much is already known on the chemistry at interfaces, clarified by key experiments and theoretical treatments. Yet there is still a considerable knowledge gap concerning the intricate dynamics of nuclei near the metallic surface. The main problem is the mechanisms of energy dissipation.¹ In metals, it is well known that a dominant source of nuclear energy dissipation is through the excitation of the electrons of the metals. A large number of theoretical models for this phenomenon has been developed for various processes on metal surfaces.^{2–18}

One particularly fundamental class of systems is the prototype process of a hydrogen atom moving towards or on a metal surface. The effect of electronic dissipation on hydrogen diffusion was studied theoretically by several groups using a variety of approaches.^{13,19–26} A particularly interesting method, appealing due to its conceptual simplicity and elegance, is the description of the atom motion via a friction coefficient.^{3,6} The friction coefficient is calculated using a carefully derived theory relying on several very reasonable assumptions, but such assumptions have not yet been fully tested. The model basically assumes that the approaching atom is slow, that the perturbation caused by its motion is weak (so that linear response theory applies), and that the energy loss occurs primarily by the low-frequency electronic excitations. Under these assumptions, the effective equation of motion for the atom can be written as

$$\mu_p \ddot{\mathbf{z}}(t) = \mathbf{F}_{\text{ad}}[\mathbf{z}(t)] + \mathbf{F}_{\text{HF}}(t) - \eta[\mathbf{z}(t)]\dot{\mathbf{z}}(t), \quad (1.1)$$

where μ_p is the proton mass, $\mathbf{z}(t)$ is the time-dependent position of the atom, and $\mathbf{F}_{\text{ad}} = -\nabla V_{\text{ad}}(\mathbf{z})$ is the adiabatic force (V_{ad} the adiabatic potential). The friction coefficient is $\eta(\mathbf{z}) = \lim_{\omega \rightarrow 0} \text{Im} \Lambda(\omega; \mathbf{z}) / \omega$, where $\Lambda(\omega; \mathbf{z})$ is the force-force correlation function at position \mathbf{z} , calculated using frequency domain linear-response time-dependent density functional theory (TDDFT) methods.⁶ $\mathbf{F}_{\text{HF}}[t; \mathbf{z}(t)]$ is a small, high-frequency, nondissipative force, depending functionally on $\mathbf{z}(t)$. The effect of this latter term is usually neglected. A more accurate description of the dissipation would include a memory kernel, yielding an effective generalized Langevin description.¹²

Our purpose in this paper is to test the friction model encapsulated in Eq. (1.1) in the case of atom–metal cluster interaction, by comparing its predictions against more rigorous calculations, in which the above-mentioned assumptions are not made. In order to assess the model for metal clusters, we launch a real-time TDDFT calculation of the atom-cluster collision using time-dependent density functional theory within the adiabatic local spin-density approximation. We believe TDDFT is appropriate for this calculation since recently it was shown able to compute nonadiabatic couplings rather accurately.²⁷ We find strong deviance from Eq. (1.1), in particular, the effective friction coefficient depends on the *direction of motion* of the atom. The friction coefficient for motion towards the cluster is much larger than that of moving away from the surface. At the turning points very strong changes in the friction coefficient are seen, but these may be of less importance because the velocity is very small.

In Sec. II, we present the details of the model and the calculation. In Sec. III we present and briefly discuss the results. A discussion and summary is presented in Sec. IV.

II. MODEL AND METHOD

An *ab initio* study of the nonadiabatic process atom-metal collision at low energies at fully realistic systems is still beyond our reach. Instead, we introduce a simpler, yet well-defined benchmark system that captures the essence of the dynamics on the one hand, and is amenable to *ab initio* treatment on the other. We hope to use in the future this system to develop useful approximations, based on these *ab initio* calculations.

The benchmark system is composed of two “classical” positively charged objects and enough quantum electrons to neutralize them. The classical objects are a proton and a large stationary ball of smeared positive charge, “jellium ball” (JB). The JB is fixed at the origin of the coordinate system and its positive charge density is radially symmetric, being near-constant, with density $n_0 = 0.022a_0^{-3}$, up to radius $R = 3.05 \text{ \AA}$. Beyond this radius the positive jellium density rapidly falls off. Such a charge profile is given by

$$n_+(\mathbf{r}) = \frac{n_0}{1 + e^{\gamma(|\mathbf{r}| - R)}}. \quad (2.1)$$

The parameter $\gamma = 3.78 \text{ \AA}^{-1}$ describes the decay slope of the positive density. The near-constant density is similar to the density of aluminum, corresponding to the Wigner-Seitz parameter $r_s = 2.2a_0$. The total charge of the JB is $Q_{\text{ball}} = 19e$. The number of electrons is $N_e = 20$. The proton is assumed to move on the z axis a distance z from the origin, thus the collision impact parameter is zero.

The Born-Oppenheimer ground-state potential surface is computed using the local density and local spin-density approximations (LDA and LSDA).^{28,29} We now briefly outline the LSDA. LDA is obtained by constraining the equality of spin-up and spin-down densities. The electronic density is assumed to be represented by Kohn-Sham (KS) orbitals $\psi_{n,s}(\mathbf{r})$, $n = 1, \dots, N_e/2$ (N_e is the number of electrons, assumed even), and $s = \uparrow, \downarrow$ designates the spin of the orbital:

$$n_s(\mathbf{r}) = \sum_{n=1}^{N_e/2} |\psi_{n,s}(\mathbf{r})|^2 \quad (s = \uparrow, \downarrow). \quad (2.2)$$

The total electronic density is the sum of spin densities:

$$n(\mathbf{r}) = n_\uparrow(\mathbf{r}) + n_\downarrow(\mathbf{r}). \quad (2.3)$$

The orbitals are obtained from the KS equation²⁸

$$-\frac{1}{2}\nabla^2\psi_{n,s} + v_s(\mathbf{r})\psi_{n,s} = \epsilon_{n,s}\psi_{n,s}. \quad (2.4)$$

Here and throughout the paper atomic units are used. The spin-polarized effective potential $v_s(\mathbf{r})$ depends on the density:

$$v_s[n_\uparrow, n_\downarrow](\mathbf{r}; \mathbf{z}) = v_H[n](\mathbf{r}) + v_+(\mathbf{r}; \mathbf{z}) + v_{xc}^s[n_\uparrow, n_\downarrow](\mathbf{r}), \quad (2.5)$$

where $v_+(\mathbf{r})$ is the electrostatic potential energy due to interaction with the static positive (“nuclear”) charges:

$$v_+(\mathbf{r}; \mathbf{z}) = -\frac{Z}{|\mathbf{r} - \mathbf{z}|} - \int \frac{n_+(\mathbf{r}')}{|\mathbf{r} - \mathbf{r}'|} d^3r'. \quad (2.6)$$

Here, Z is the hydrogen charge ($Z=1$ in our units) and $n_+(\mathbf{r})$ is the positive charge density of the jellium sphere [see Eq. (2.1)]. $v_H[n](\mathbf{r})$ is the repulsive electrostatic potential energy due to interaction of an electron with the electronic charge density $n(\mathbf{r}) = n_\uparrow(\mathbf{r}) + n_\downarrow(\mathbf{r})$:

$$v_H[n](\mathbf{r}) = \int \frac{n(\mathbf{r}')}{|\mathbf{r} - \mathbf{r}'|} d^3r'. \quad (2.7)$$

Finally, the exchange-correlation potential is given by

$$v_{xc}^s[n_\uparrow, n_\downarrow](\mathbf{r}) = \frac{d}{dn_s} \{n_s(\mathbf{r}) \epsilon_{xc}[n_\uparrow(\mathbf{r}), n_\downarrow(\mathbf{r})]\}, \quad (2.8)$$

where $\epsilon_{xc}(n_\uparrow, n_\downarrow)$ is the energy per particle of the homogeneous electron gas (we use the parametrization of Ref. 30). Equation (2.4) must be solved self-consistently with Eqs. (2.2) and (2.5). Once this is achieved, the Born-Oppenheimer energy curve $V_{\text{ad}}(\mathbf{z})$ is then simply the total energy of a stationary proton situated at distance z from the origin:

$$V_{\text{ad}}(\mathbf{z}) = E_{\text{el}}(\mathbf{z}) + Z \int \frac{n_+(\mathbf{r}')}{|\mathbf{r}' - \mathbf{z}|} d^3r', \quad (2.9)$$

where the electronic energy is

$$\begin{aligned} E_{\text{el}}(\mathbf{z}) &= \sum_{n=1}^{N_e} \langle \psi_n | -\frac{1}{2}\nabla^2 + v_+(\mathbf{r}; \mathbf{z}) | \psi_n \rangle \\ &+ \frac{1}{2} \int \frac{n(\mathbf{r})n(\mathbf{r}')}{|\mathbf{r} - \mathbf{r}'|} d^3r d^3r' \\ &+ \int n(\mathbf{r}) \epsilon_{xc}[n_\uparrow(\mathbf{r}), n_\downarrow(\mathbf{r})] d^3r. \end{aligned} \quad (2.10)$$

The adiabatic force on the nucleus is derived from V_{ad} :

$$\mathbf{F}_{\text{ad}}(\mathbf{z}) = \int \mathbf{E}(\mathbf{r}' - \mathbf{z}) [n_+(\mathbf{r}') - n(\mathbf{r}')] d^3r', \quad (2.11)$$

where

$$\mathbf{E}(\mathbf{r}) = Z \frac{\mathbf{r}}{r^3} \quad (2.12)$$

is the electric field of the proton.

Next, we discuss the dynamics of the proton and the electrons. When a hydrogen atom collides with a jellium sphere, the electrons must react to its motion. The ensuing dynamics is very complex. We use the Ehrenfest molecular dynamics approach,^{31,32} assuming that the nucleus is classical, leading to the following equation of motion for the nucleus:

$$\mu_p \ddot{\mathbf{z}} = \int \mathbf{E}(\mathbf{r}' - \mathbf{z}) [n_+(\mathbf{r}') - n(\mathbf{r}', t)] d^3r', \quad (2.13)$$

where μ_p is the mass of the proton. Here, the time dependent electron density $n(\mathbf{r}, t)$ is calculated using time-dependent density functional theory, in the adiabatic local spin-density approximation.³³ This is done by solving the time-dependent Kohn-Sham equations:

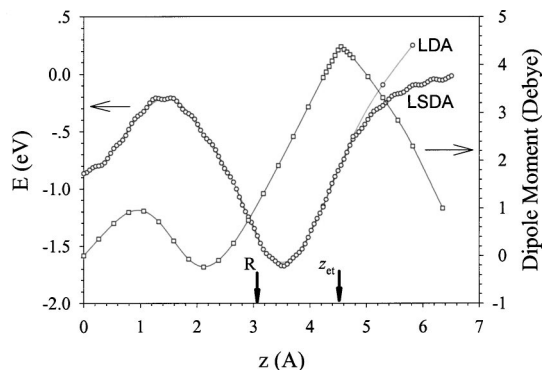


FIG. 1. The adiabatic potential energy curves (circles) and electric dipole moment (squares) vs distance z of the H+JB system. Lines connect the calculated values. Both LSDA and LDA based potential curves are shown. The R and z_{et} arrows designate the location of the surface and the electron transfer point, respectively.

$$i \frac{\partial \psi_{n,x}(\mathbf{r}, t)}{\partial t} = -\frac{1}{2} \nabla^2 \psi_{n,s}(\mathbf{r}, t) + v_s[\mathbf{r}; \mathbf{z}(t)] \psi_{n,s}(\mathbf{r}, t), \quad (2.14)$$

where $v_s[n_\uparrow, n_\downarrow](\mathbf{r}, \mathbf{z})$ is given by Eq. (2.5). Equation (2.14) is implemented using a plane-wave basis^{34,35} and pseudopotential,³⁶ with cutoff energy of $11E_h$ and a cubic cell size of $32a_0$. It was assumed throughout that the z component of the spin is unpolarized ($S_z=0$).³⁷ The time propagation is done with a fifth-order adaptive Runge-Kutta method³⁸ concurrently with the position and velocity of the proton [Eq. (2.13)], propagated using the velocity-Verlet method, with time step of $\Delta t = 0.5\hbar E_h^{-1}$. The real-time approach to time-dependent adiabatic LDA and LSDA have been shown a useful tool for analyzing a variety of molecular electron dynamics problems.^{27,39-43} Recently, a new method was developed for including nonadiabatic⁴⁴ effects in the exchange correlation effects.^{45,46}

III. RESULTS

We first computed the ground state potential energy of the proton as a function of its distance z from the center of the cluster. Two related approaches were used, briefly described in the preceding section, the LSDA and the LDA. The results are shown in Fig. 1. For small distances ($z < 5 \text{ \AA}$) LDA and LSDA give identical energies. However, when the bond is broken, LDA exhibits an erroneous asymptotic energy. The failure of LDA in breaking bonds is well known and we therefore work only with LSDA. We checked that LSDA converges to the limit of a hydrogen atom infinitely separated from a neutral jellium sphere (by computing the individual energies of the two entities).

Within LSDA, the bond energy is 1.57 eV. The bond equilibrium distance is $Z_{eq} = 3.7 \text{ \AA}$, corresponding to a height $h_{eq} = Z_{eq} - R = 0.65 \text{ \AA}$ above the metal surface. It is interesting to find that a metastable state of the hydrogen situated in the center of the sphere exists.

The radial component of the total electric dipole moment $\mathbf{d} = \int \mathbf{n}(\mathbf{r}) \mathbf{r} d^3r - Z\mathbf{z}$ teaches us more on the electronic structure. At infinite separation, it is clear that at this limit each entity has zero moment ($\mathbf{d} \rightarrow 0$). When the atom is at the

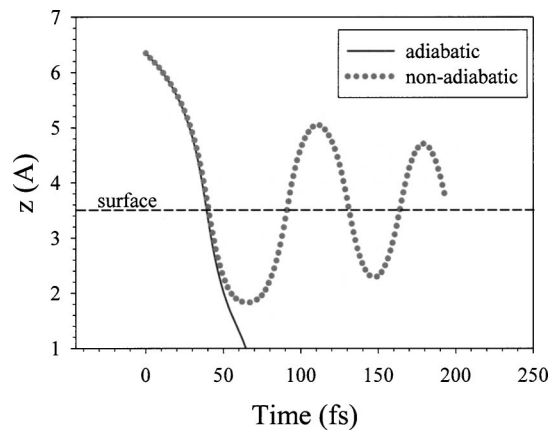


FIG. 2. The trajectory of the hydrogen atom for the adiabatic and nonadiabatic dynamics. The damped oscillator character is evident.

center of the jellium, then by symmetry $\mathbf{d}=0$. In between these limits the dipole moment is shown in Fig. 1. It exhibits a maximum at $z_{et} = 4.55 \text{ \AA}$, with a dipole moment of 4.4 D. The maximum is very similar in shape to a cusp, indicating the point of occurrence of an electron transfer from the metal to the atom. At this point we may argue that the atom's affinity level drops below the Fermi energy of the metal. The dipole moment becomes slightly negative at $z = 2 \text{ \AA}$.

The dynamics is studied next. We place the proton at an initial position far from the JB ($z_0 = 6.35 \text{ \AA}$). The electronic state is assumed to be the ground state. The atom is given a small initial kinetic energy, of $E_{k,0} = 0.052 \text{ eV}$, with velocity directed towards the center of the JB along the z axis. With this kinetic energy the total adiabatic energy of the atom is zero. The resulting dynamics is collinear along the z axis.

The position of the hydrogen atom as a function of time is calculated by the method discussed in the preceding section and shown in Fig. 2. The atom has enough initial energy to go through the jellium cluster, had its motion been adiabatic (see the adiabatic trajectory in Fig. 2). However, due to the friction it is effectively trapped at the surface of the cluster, showing damped oscillations of recollisions. The energy of the atom,

$$E_{\text{atom}}[z(t)] = \left(\frac{1}{2} \mu_p \dot{z}(t)^2 + V_{\text{ad}}[z(t)] \right), \quad (3.1)$$

is damped at each recollision, as shown in Fig. 3. The dissipation is especially strong when the atom moves towards the surface.

For the purpose of analyzing the friction model we time-average the instantaneous nonadiabatic force, eliminating F_{HF} , and obtaining an effective friction coefficient

$$-\eta[z(t)] = \frac{\overline{\mu_p \ddot{z}(t) - F_{\text{ad}}[z(t)]}}{v(t)} \equiv \frac{\overline{\Delta F(t)}}{v(t)}, \quad (3.2)$$

where

$$\overline{\Delta F(t)} = \frac{1}{\sqrt{2\pi\sigma}} \int_{-\infty}^{\infty} \Delta F(\tau) e^{(t-\tau)^2/2\sigma^2} d\tau, \quad (3.3)$$

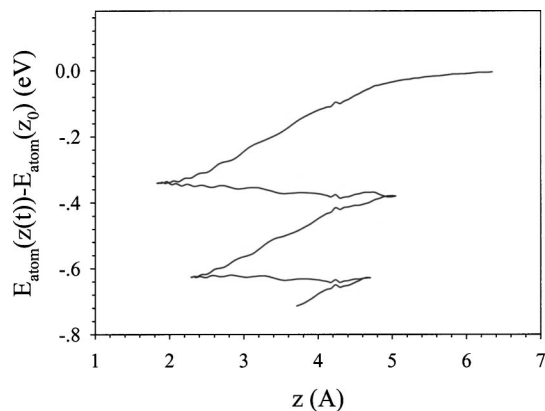


FIG. 3. The energy loss of the proton along the trajectory.

and the averaging time is taken to be $\sigma=10$ fs. It is seen in Fig. 2 that during the averaging interval the atom moves only a small distance. The high-frequency force

$$F_{\text{HF}}(t) = \Delta F(t) - \overline{\Delta F}(t) \quad (3.4)$$

is shown in Fig. 4, superimposed on the adiabatic force. The latter exhibits oscillations due to the corrugation of the adiabatic potential surface, as seen in Fig. 1. The highest frequencies are seen when the atom reaches its turning point at $z \approx 1.9 \text{ \AA}$. A somewhat strong oscillation is visible at $z = 4.2 \text{ \AA}$; at this location, a small perturbation to the energy loss curve (Fig. 3) is noticed. This effect will be discussed further in the following section. The amplitude of oscillations is around 0.005 a.u. of force, usually much smaller than the adiabatic force, except near extreme points of the potential curve.

The effective friction coefficient is shown in Fig. 5. It is seen that as the atom starts from $z = 6 \text{ \AA}$, the coefficient is small and it grows until it reaches the value of $\sim 0.7 \text{ meV ps \AA}^{-2}$; it then decreases slightly as the atom enters the higher density region, reaching $\sim 0.9 \text{ meV ps \AA}^{-2}$. At the inner turning point the effective friction coefficient drops steeply, reaching negative values. At these points the velocity changes sign and the validity of our method to extract the friction coefficient (or perhaps its very definition) is questionable. As the atom returns, the effective friction coefficient

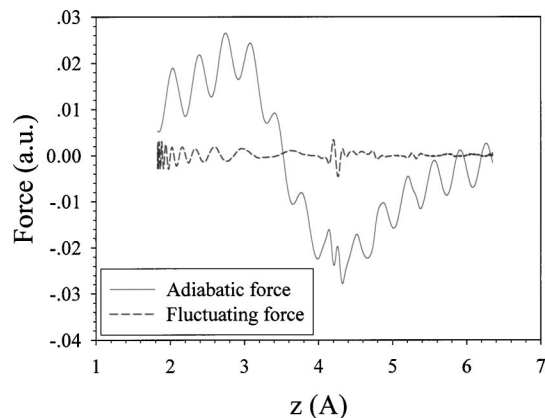


FIG. 4. The fluctuating force (dashed), as a result of the electronic excitations, superimposed on the adiabatic force (full).

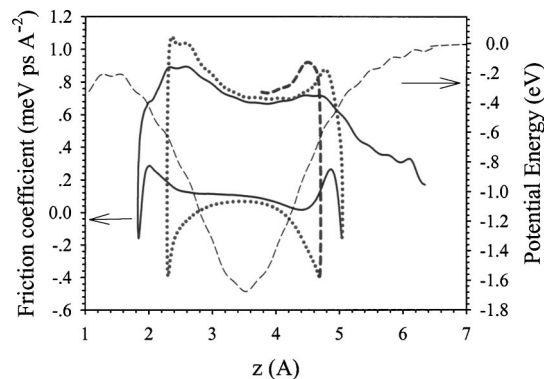


FIG. 5. The effective friction coefficient along the nuclear trajectory. First round (full), second round (dotted), and beginning of third round (dashed), superimposed—the adiabatic potential (dashed).

is seen to be considerably smaller than that of the incoming motion. The qualitative behavior in the second and third periods is similar to the first.

IV. DISCUSSION AND SUMMARY

We have applied an *ab initio* calculation to study the dynamics of the collision of a hydrogen atom with a metal cluster, a JB. While the model for the metal is simplistic, it still allows to focus on the role of electronic excitations in a realistic way. We find, in accordance with accepted views, that the motion of the atom is indeed similar to that of a damped oscillator under friction.

However, new phenomena emerge quite clearly. The friction coefficient seems to depend on the direction of motion, unexpected in present models. One goal for future research is to clarify the reasons for this behavior. To attribute the friction to the “direction of motion” is oversimplistic, and perhaps misleading. Analysis of the Ehrenfest molecular mechanics shows that if t_1 and t_2 are two times for which $\mathbf{z}(t_1) = \mathbf{z}(t_2) \equiv \mathbf{z}$ and $\dot{\mathbf{z}}(t_1) \approx -\dot{\mathbf{z}}(t_2) \equiv \mathbf{v}$, then from Eqs. (3.2) and (2.13):

$$\Delta \eta_{21} = \frac{\int \mathbf{E}(\mathbf{r}' - \mathbf{z}) [n(\mathbf{r}', t_1) - n(\mathbf{r}', t_2)] d^3 r'}{|\mathbf{v}|}. \quad (4.1)$$

This formula shows that the difference in friction can be attributed to the fact that the electrons have different densities at the two different times. Thus, in this picture, the change in the friction coefficient can be attributed to a “memory effect,” since the electronic state is evidently sensitive to the history of the dynamics.

Another issue is the role the electron transfer point, which occurs at the dipole moment cusp, $z_{\text{et}} = 4.55 \text{ \AA}$. At this point a large maximal peak in the friction coefficient is observed in the linear response calculation.²⁶ In our calculation, the maximal peak is shifted to a somewhat further distance: $z \approx 4.8 \text{ \AA}$ at the first crossing and at later crossings the maximum is shifted at first to larger and then to smaller distances. The peak is smeared on the first approach, while on the second and third recollisions it is more distinct. Additionally, near the inner turning points, at $z = 2 - 2.2 \text{ \AA}$, the position of the minimum of the dipole moment, there is a second peak. A different phenomenon worth mentioning is that at distance

slightly below the crossing, at $z=4.2 \text{ \AA}$, there is a seemingly resonance effect, manifested as a peak in the high-frequency force (Fig. 4) and the energy loss spectrum (Fig. 3). This effect seems velocity independent.

Summarizing, we have studied, using real-time *ab initio* methods the collision of a hydrogen atom and a metal cluster and found that the phenomenological friction coefficient strongly depends on the direction of the motion of the atom. The high-frequency force is usually very small, but is noticeable at the electron transfer point and at the turning points of the atom trajectory. Several other differences from previous related work were pointed out. Further studies will attempt to construct a simple model that accounts for these findings.

ACKNOWLEDGMENTS

The idea for this study originates in a lecture given by S. Holloway during the Ein-Gedi 2004 conference organized by Professors M. Asscher, R. Kosloff, and Y. Zeiri. We gratefully acknowledge the support of the Israel-German foundation (GIF).

- ¹J. C. Tully, *Annu. Rev. Phys. Chem.* **51**, 153 (2000).
- ²J. W. Gadzuk and A. C. Luntz, *Surf. Sci.* **144**, 429 (1984).
- ³E. G. d'Agliano, P. Kumar, W. Schaich, and H. Suhl, *Phys. Rev. B* **11**, 2122 (1975).
- ⁴K.-P. Bohnen, M. Kiwi, and H. Suhl, *Phys. Rev. Lett.* **34**, 1512 (1975).
- ⁵W. L. Schaich, *Surf. Sci.* **49**, 221 (1975).
- ⁶B. Hellsing and M. Persson, *Phys. Scr.* **29**, 360 (1984).
- ⁷D. C. Langreth, *Phys. Rev. Lett.* **54**, 126 (1985).
- ⁸G. Wahnstrom, *Chem. Phys. Lett.* **163**, 401 (1989).
- ⁹Y. G. Li and G. Wahnstrom, *Phys. Rev. Lett.* **68**, 3444 (1992).
- ¹⁰E. Blaistenbarojas and J. W. Gadzuk, *J. Chem. Phys.* **97**, 862 (1992).
- ¹¹P. Saalfrank, R. Baer, and R. Kosloff, *Chem. Phys. Lett.* **230**, 463 (1994).
- ¹²M. Head-Gordon and J. C. Tully, *J. Chem. Phys.* **103**, 10137 (1995).
- ¹³R. Baer and R. Kosloff, *J. Chem. Phys.* **106**, 8862 (1997).
- ¹⁴G. K. Paramonov and P. Saalfrank, *J. Chem. Phys.* **110**, 6500 (1999).
- ¹⁵M. Plihal and D. C. Langreth, *Phys. Rev. B* **60**, 5969 (1999).
- ¹⁶B. N. J. Persson and J. W. Gadzuk, *Surf. Sci.* **410**, L779 (1998).
- ¹⁷S. K. Mengel and G. D. Billing, *J. Phys. Chem. B* **101**, 10781 (1997).
- ¹⁸G. R. Darling and S. Holloway, *Rep. Prog. Phys.* **58**, 1595 (1995).
- ¹⁹Y. C. Sun and G. A. Voth, *J. Chem. Phys.* **98**, 7451 (1993).
- ²⁰T. Miyake, K. Kusakabe, and S. Tsuneyuki, *Surf. Sci.* **363**, 403 (1996).
- ²¹R. Baer, Y. Zeiri, and R. Kosloff, *Phys. Rev. B* **55**, 10952 (1997).
- ²²T. R. Mattsson and G. Wahnstrom, *Phys. Rev. B* **56**, 14944 (1997).
- ²³T. R. Mattsson, G. Wahnstrom, L. Bengtsson, and B. Hammer, *Phys. Rev. B* **56**, 2258 (1997).
- ²⁴R. Baer, Y. Zeiri, and R. Kosloff, *Surf. Sci.* **411**, L783 (1998).
- ²⁵J. R. Trail, M. C. Graharn, and D. M. Bird, *Comput. Phys. Commun.* **137**, 163 (2001).
- ²⁶J. R. Trail, D. M. Bird, M. Persson, and S. Holloway, *J. Chem. Phys.* **119**, 4539 (2003).
- ²⁷R. Baer, *Chem. Phys. Lett.* **264**, 75 (2002).
- ²⁸W. Kohn and L. J. Sham, *Phys. Rev. A* **140**, A1133 (1965).
- ²⁹O. Gunnarsson and B. I. Lundqvist, *Phys. Rev. B* **13**, 4274 (1976).
- ³⁰J. P. Perdew and Y. Wang, *Phys. Rev. B* **45**, 13244 (1992).
- ³¹P. Ehrenfest, *Z. Phys.* **45** (1927).
- ³²J. Theilhaber, *Phys. Rev. B* **46**, 12990 (1992).
- ³³E. Runge and E. K. U. Gross, *Phys. Rev. Lett.* **52**, 997 (1984).
- ³⁴M. C. Payne, M. P. Teter, D. C. Allan, T. A. Arias, and J. D. Joannopoulos, *Rev. Mod. Phys.* **64**, 1045 (1992).
- ³⁵G. J. Martyna and M. E. Tuckerman, *J. Chem. Phys.* **110**, 2810 (1999).
- ³⁶N. Troullier and J. L. Martins, *Phys. Rev. B* **43**, 1993 (1991).
- ³⁷Since we are working within LSDA, we are in fact allowing spin relaxation, by decoupling the up- and down-spin densities.
- ³⁸W. H. Press, S. A. Teukolsky, W. T. Vetterling, and B. P. Flannery, *Numerical Recipes in C* (Cambridge University Press, Cambridge, 1992).
- ³⁹R. Baer, S. Weiss, and D. Neuhauser, *Nano Lett.* **4**, 85 (2004).
- ⁴⁰R. Baer, T. Seideman, S. Ilani, and D. Neuhauser, *J. Chem. Phys.* **120**, 3387 (2003).
- ⁴¹R. Baer, D. Neuhauser, P. Zdanska, and N. Moiseyev, *Phys. Rev. A* **68**, 043406 (2003).
- ⁴²R. Baer and R. Gould, *J. Chem. Phys.* **114**, 3385 (2001).
- ⁴³R. Baer and D. Neuhauser, *Int. J. Quantum Chem.* **91**, 524 (2003).
- ⁴⁴It is important to distinguish between the nonadiabatic effects of the nuclear motion (with respect to the Born-Oppenheimer approximation) and the nonadiabatic approximation in the exchange-correlation potentials.
- ⁴⁵Y. Kurzweil and R. Baer, *J. Chem. Phys.* (in press) 2004.
- ⁴⁶J. F. Dobson, M. J. Bunker, and E. K. U. Gross, *Phys. Rev. Lett.* **79**, 1905 (1997).